Inorganic Chemistry, Vol. 16, No. 12, 1977 **3013**

Contribution from the Department of Inorganic Chemistry, The University, Newcastle upon Tyne, NE1 7RU, England

Substitution Reactions at Square-Planar d^8 Metal Centers and the Kinetic Cis and Trans Effects. A General Molecular Orbital Description

JEREMY K. BURDETT

Received April 26, 1977 AIC70285D

The angular overlap model of transition-metal ligand interaction is used to derive for the first time a double-humped potential-energy surface for the substitution of a simple ligand in a low-spin d^8 square-planar transition-metal complex. The potential surface in general contains a transition state, mainly associated with bond making, a trigonal-bipyramidal intermediate, and a transition state, mainly associated with bond breaking. The energies of the turning points of this potential surface are readily expressible in terms of the σ and π properties of the ligands and the size of the interaction of the entering or leaving ligand with $(n + 1)$s,p orbitals on the metal. The height of the entering barrier is found to dominate the rate in a large number of cases. This barrier height decreases and thus rate of reaction increases with (a) increasing σ strength of entering ligand, (b) π acceptor orbitals on entering ligand, (c) good interaction with $(n + 1)$s,p orbitals on metal by entering ligand, (d) entering ligand "softness", (e) decreasing σ strength of trans ligand (the trans-labilizing influence), (f) decreasing σ strength of leaving ligand, and (g) increasing σ strength of cis ligands (cis effect). The relative leaving barrier heights determine which ligand is lost from the tbp intermediate. The barrier height increases (and therefore trans-directing influence increases) with (a) decreasing σ donor strength of trans ligand, (b) π acceptor strength of trans ligand, (c) good interaction of trans ligand with $(n + 1)$s,p orbitals on metal, and (d) "softness" of trans ligand. These two sets of properties match quite well those deduced from experiment. Substitution of numerical values (taken from electronic spectral measurements) for the σ strengths of the ligand concerned into expressions describing the barrier heights give excellent correlation with experimentally measured values of the rate constants for the hydrolysis, ammoniolysis, and anation reactions of $Pt(NH_3)_x(H_2O)_yCl_{4-x-y}$ systems and related molecules.

Introduction

The substitution reactions of low-spin d^8 square-planar complexes have been well studied, especially for those cases where the reactions are slow enough to be conveniently followed as is the case with Pt^{II}. The general rate law for ligand substitution is a two-part one for attack of Y (eq 1). There

$$\text{rate} = (k_1 + k_2[Y])[\text{substrate}] \quad (1)$$

is excellent evidence that the k_2 route is a simple displacement mechanism proceeding via a trigonal-bipyramidal-based moiety (I) in which the entering ligand occupies an equatorial site.

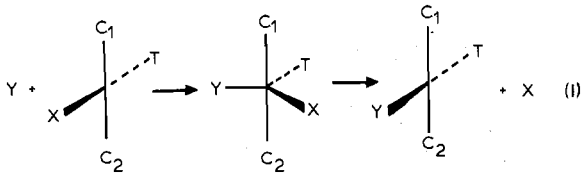

(I)

The experimental data have been extensively reviewed.[1-10] The k_1 route is via a solvent (S)-assisted mechanism (eq 2). Under

$$MC_1C_2XT \xrightarrow[S]{\text{slow}} MC_1C_2ST \xrightarrow[Y]{\text{fast}} MC_1C_2YT \quad (2)$$

certain conditions there is experimental evidence for dimeric intermediates[11] which will not concern us here. We shall be concerned with the bimolecular path indicated by I which describes the rate-determining step in the k_1 pathway (with Y = S) as well as the k_2 route. One often dramatic feature of the process is the role of the ligand T, trans to the replaceable group X in the planar substrate. The course and rate of the reaction are dependent upon the nature of the ligand T in two main ways. First, there is the "trans-directing influence", the part played by the ligand T in deciding which ligand (X or T) is replaced. Second, there is the "trans-labilizing effect", the effect of T on the rate of ligand substitution. These observations we collectively term the "trans effect". In addition, the cis ligands C_1 and C_2 may sometimes play a significant role in the course and rate of the replacement process. Usually however this "cis effect" is smaller than the trans effect. (A parallel series of observations on the perturbation of MX bond lengths, vibrational stretching frequencies, etc., by the trans ligand T is also well-known (see, for example, ref 9) for the square-planar complex itself. We follow modern practice[12] and call this static phenomenon the "trans influence". The two, trans effect and trans influence, may or may not be related.) Examination of a large number of displacement reactions gives us a trans-effect order which is approximately

$$T = CO, CN, C_2H_4 > PR_3, H^- > CH_3^-, \text{thiourea} > NO_2^-, I^-, SCN^- > Br^- > Cl^- > py > NH_3 > H_2O > OH^- \quad (3)$$

This is the order of decreasing trans-labilizing effect or decreasing trans-directing influence. There are however several exceptions to this order and one particularly interesting set of observations where for strong nucleophiles (I^-, thiourea, etc.) as entering groups this trans-effect order is reversed.[13] There is a large amount of experimental data in this field. However, conclusions drawn from one small group of reactions often do not seem to hold when transferred to another system. The largest set of available *systematic* studies which we shall examine are the hydrolysis, ammoniolysis, and anation reactions of $Pt(H_2O)_x(NH_3)_yCl_{4-x-y}$ and related DMSO systems. These we feel will give a much more reliable test of the theory than the collation of the rather fragmentary (and often contradictory as we have just noted) information from other systems. In this paper we shall use a simple molecular orbital model to reproduce some of the more general features observed in these d^8 replacement reactions. While relatively crude we hope it will provide a basis for construction of an experimental strategy with which to tackle the problem further and perhaps a spur to further theoretical development.

Theoretical Approaches

Theoretically, most studies have centered around the reaction profile of Figure 1a containing a trigonal-bipyramidal transition state.[14] Several authors have discussed the influence of the properties of the ligand T on the energy separation between planar substrate and entering ligand and this proposed trigonal-bipyramidal transition state (I). In molecular orbital terms this activation energy for reaction is lowered if there is strong σ bonding between the ligand T and the metal $(n + 1)$p or $(n + 1)$s orbitals.[2,15-17] Using overlap considerations[15] it seems possible to rationalize the ordering in that part of the trans-effect series where σ bonding is expected to be the major force involved on this basis. As far as π acceptors are concerned, it has been argued[18,19] that these ligands, present in

Table I. Experimentally Determined Values (μm^{-1}) of σ and π Parameters for Cr^{III} Complexes[a] from Reference 29

X	NH_3	py	H_2O	F^-	Cl^-	Br^-	OH^-
$\beta_\sigma(X)S_\sigma^2(X)$	0.704 ± 0.002	0.585 ± 0.009	0.79 ± 0.06	0.739 ± 0.007	5.54 ± 0.14	0.492 ± 0.009	~0.867
$\beta_\pi(X)S_\pi^2(X)$	0[b]	−0.050 ± 0.005	0.19 ± 0.05	0.169 ± 0.003	0.87 ± 0.11	0.063 ± 0.01	~0.225

[a] These values are related to those of ref 29 by $\Delta_\sigma = 3\beta_\sigma S_\sigma^2$ and $\Delta_\pi = 4\beta_\pi S_\pi^2$. [b] Values relative to $\beta_\pi(NH_3)S_\pi^2(NH_3) = 0$.

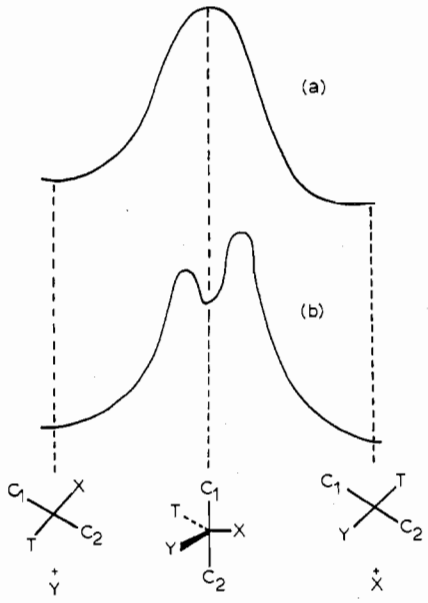

Figure 1. Reaction coordinate energy profile for (a) the tbp transition state and (b) the tbp intermediate.

the complex, absorb some of the excess negative charge introduced by the entering group and hence lower the energy of the trigonal-bipyramidal (tbp) transition state.

Therefore good overlap with metal $(n + 1)$s, p orbitals or π-acceptor character makes for a good labilizer but this model obviously does not allow us to decide upon trans-directing ability, i.e., which ligand is preferentially ejected from the tbp transition state. The activation energy of Figure 1a has also been approached using a d orbital only model via the angular overlap method.[20,21] The ligand-field contribution to the activation energy has been obtained in a parametrized form as a function of the σ and π properties of the coordinated ligands and is able to view successfully the trends in rate constants in a series of related reactions. We return to this particular theoretical advance below. The method has the drawback that it is also unable to comment on the trans-directing influence of the ligand T since it is still limited by the form of the profile of Figure 1a. Quantitative molecular orbital calculations aimed at predicting the most favored decomposition route of the tbp (loss of X, Y, or T) have used the assumption that the ligand most likely to be ejected is the one where the largest reduction in metal–ligand bond overlap population occurs on going from the planar substrate to tbp transition state. Depending upon the parametrization of the molecular orbital method $(n + 1)$s and $(n + 1)$p orbitals are of either vital[16] or little[17] importance in determining which ligand is lost. The real situation here is far from clear at present.

A potential surface more realistic than Figure 1a for this displacement process is shown in Figure 1b where the tbp may be an intermediate and there are transition states associated with the bond making and breaking processes. It is generally considered that a surface of this type will be needed to really understand the various nuances of these displacement reactions. Until now, such a surface has not been generated theoretically. Below we derive such a potential surface in terms of the π and σ properties of the coordinated ligands and thus are able to see how the various barriers to reaction along the coordinate of Figure 1b are sensitive to the nature of the various entities involved in the chemistry.

The Angular Overlap Model of Transition-Metal–Ligand Interaction

Since it is vital in understanding what follows we give a brief discussion of the theoretical model we shall use, deriving along the way energies of the relevant orbitals and structures needed later. The angular overlap model[22-25] provides basically one thing, the energies of the (mainly) transition-metal d orbitals (relative to the naked uncoordinated M atom or ion) in an ML_n complex of given geometry in terms of two parameters (like the Δ or Dq of crystal field theory). It is based on the assumption that to a first approximation the interaction energy ϵ of two orbitals ϕ_i and ϕ_j on two different centers is proportional to the square of the overlap integral between them, $\epsilon = \beta S_{ij}^2$. In our case here ϕ_i is a central atom (metal) d orbital and ϕ_j is either a single ligand orbital or a symmetry adapted combination of ligand orbitals. We assume that the total interaction energy of an orbital ϕ_i with the ligands X is the sum of all the individual interactions,[26] i.e.

$$\epsilon = \sum_j \beta_\lambda(X) S_{ij}^2(X;\lambda) \tag{3a}$$

where a different value of the proportionality constant is included for $\lambda = \sigma,\pi$ type interactions. The beauty of the scheme lies in the fact that for a given metal–ligand distance the overlap integral is just a function of the polar coordinates (θ,ϕ) describing the ligand position, i.e.

$$S = S_\lambda f(\theta,\phi) \tag{4}$$

We give some useful values of the angular dependence of these overlap integrals in II. A complete set for s, p, d, and f orbitals

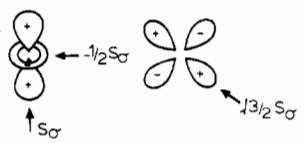

(II)

is given in ref 27. Thus the total interaction energy associated with a particular metal d orbital is the sum of a series of terms of the sort $\beta_\sigma(X)S_\sigma^2(X)$ and $\beta_\pi(X)\,S_\pi^2(X)$ representing σ and π effects, respectively. We then have a two (one for σ and one for π) parameter model. From the analysis of the electronic spectra of several Cr^{III} systems, values of these parameters have been experimentally determined for a limited series of π-donor ligands (Table I).

Using eq 2 we may readily calculate the interaction energies of the ligands and metal d orbitals. Figure 2 gives the d-orbital region of the molecular-orbital diagram for square-planar and trigonal-bipyramidal complexes, along with the corresponding levels of the ligand σ and π orbitals. We have replaced the rather cumbersome terms $\beta_\sigma(X)S_\sigma^2(X)$ and $\beta_\pi(X)S_\pi^2(X)$ by X_σ and X_π, respectively. An interesting sum rule applies to these molecular-orbital diagrams. Interaction energies associated with all of the d orbitals (or their ligand-located counterparts) are equal to $\sum n_X\beta_\sigma(X)S_\sigma^2(X)$ where n_X is the number of ligands X present. A similar equation applies for π-type interactions. Two distinct cases arise in the systems under examination here: one where the ligands are π acceptors (Figure 2a) and the other where they are π donors (Figure

Table II. Molecular-Orbital Stabilization Energies for d^8 Planar and tbp Structures

Planar MC_1C_2XT	$3/2(C_{1\sigma} + C_{2\sigma} + X_\sigma + T_\sigma) + \Sigma_L(L_s + 4L_\pi)$
tbp(I) $M(C_1C_2)(XYT)$	$2C_{1\sigma} + 2C_{2\sigma} + {}^1/_2X_\sigma + {}^1/_2Y_\sigma + {}^1/_2T_\sigma + \Sigma_L(L_s + 4L_\pi)$
tbp(II) $M(XT)(C_1C_2Y)$	$2X_\sigma + 2T_\sigma + {}^1/_2C_{2\sigma} + {}^1/_2C_{2\sigma} + {}^1/_2Y_\sigma + \Sigma_L(L_s + 4L_\pi)$
Δ, difference planar – tbp(I)	$-{}^1/_2C_{1\sigma} - {}^1/_2C_{2\sigma} - {}^1/_2Y_\sigma + X_\sigma + T_\sigma - 4Y_\pi - Y_s$
difference planar – tbp(II)	$-{}^1/_2X_\sigma - {}^1/_2T_\sigma - {}^1/_2Y_\sigma + C_{1\sigma} + C_{2\sigma} - 4Y_\pi - Y_s$

2b). In the former case the metal d orbitals are stabilized by π interaction and in the latter they are destabilized. In the case of ligands which are σ and π donors the metal-centered orbitals are of course metal–ligand antibonding. There exist to lower energy (shown in detail in Figure 2a and b) completely filled metal–ligand bonding orbitals, which are mainly ligand located, each of which has a metal-centered M–L antibonding counterpart. Thus in these low-spin d^8 complexes the total molecular-orbital stabilization energy is simply the stabilization energy afforded the two electrons in the most deeply bound bonding orbital whose M–L antibonding counterpart (mainly metal d orbital) is unoccupied. The stabilization energy contributed by electrons in all other (ligand located) M–L bonding orbitals is offset by occupation of their M–L antibonding counterparts.[25,30] Assuming that the destabilization energy of the antibonding orbital is the same as the stabilization energy of its bonding partner then the total molecular-orbital stabilization energy of the molecule is simply

$$\Sigma(\sigma) = 2\sum_X \beta_\sigma(X)S^2(X;\sigma) \quad (5)$$

where the overlap integrals are between the highest energy d orbital ($d_{x^2-y^2}$ in the planar substrate, d_{z^2} in the tbp) and the ligand orbitals. In this case we see with this particular d-orbital configuration π donor effects of the ligands do not contribute to the stabilization energy of either structure. For the case of π acceptors we need to add to $\sum(\sigma)$ of eq 5 a contribution $\sum(\pi)$ to allow for the fact that in contrast to the above, the metal–ligand π-bonding orbitals are filled (Figure 2b). These are mainly metal-centered d orbitals whereas their antibonding partners are unoccupied. This term from the sum rule is simply

$$\Sigma(\pi) = 2\sum_X M_X\beta_\pi(X)S_\pi{}^2(X) \quad (6)$$

(where M_X is the number of π acceptor orbitals (1 or 2) borne by the ligand X) for the systems under consideration since all metal–ligand π-bonding orbitals are occupied. The orbitals $d_{x^2-y^2}$ (planar) and d_{z^2} (tbp) are involved in σ interactions only.

The interactions of the ligands with $(n + 1)$s and $(n + 1)$p orbitals on the metal atom also make a sizable contribution to the overall strength of the metal–ligand bond,[31] and we will find that these d^8 replacement processes may not be understood by using metal d orbitals alone. The orbitals which contain large metal–ligand bonding contributions via such interactions are mainly ligand-located orbitals containing the M(d)–L bonding interactions. In contrast to the d orbital interactions, the M–L antibonding orbitals produced via interactions with these higher energy metal orbitals are of course mainly metal-located $(n + 1)$s, $(n + 1)$p orbitals and are unoccupied. Under these circumstances by making use of the sum rule mentioned above the total stabilization energy from this source *whatever the geometry* is from each ligand.

$$Y_s = 2\beta_s(Y)S_s{}^2(Y) + 2\beta_p(Y)S_p{}^2(Y) \quad (7)$$

Armed with eq 5, 6, and 7 we may rapidly proceed to derive the total molecular-orbital stabilization energies associated with metal–ligand interactions for the planar substrate and two possible tbp geometries approachable in one step from the planar molecule (Table II). We notice one very striking result; the π properties of all the ligands except the entering one do not appear in the expression for the energy difference between the two structures. It is in addition only the π *acceptor* properties of the entering ligand which are important. Similarly, on this simple approach the only ligand which will have a contribution to make to the differential stabilization of planar substrate and tbp intermediate via interaction with metal $(n + 1)$s,p orbitals is the entering one.

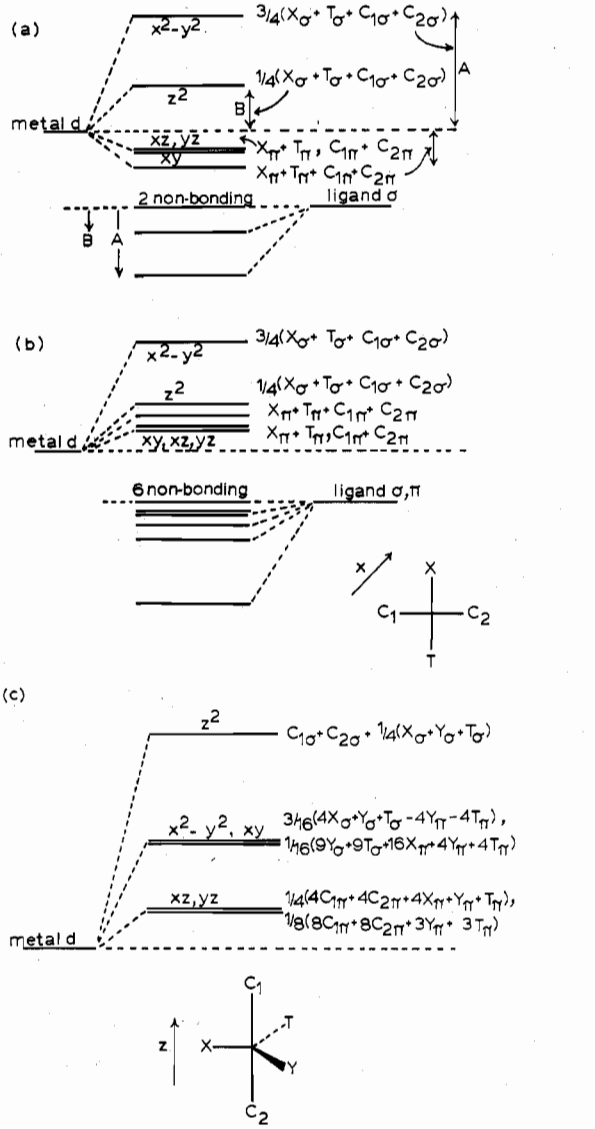

Figure 2. Molecular-orbital splitting patterns on a d orbital only model in square-planar and tbp geometries. (a) The square-planar system with π-acceptor ligands. (Here the two nonbonding orbitals will in fact be depressed in energy due to interaction with $(n + 1)$s,p orbitals on the metal.) The total d-orbital stabilization energy for the low-spin d^8 system is simply 2A. (b) The square-planar system with π-donor ligands. (The six nonbonding orbitals may interact with the metal $(n + 1)$s,p orbitals.) The quantitative splittings of the bonding orbitals are the mirror image of the splittings associated with the d orbitals. (c) The trigonal bipyramid with π-donor ligands. The d-orbital region only is shown here. In all these diagrams a comma separates the energies of the energy levels which are degenerate in the ML_4 or ML_5 case with identical ligands.

At this stage we take the opportunity to comment on a line of reasoning often used[32] to view the differential stabilization

effect associated with ligand interactions with metal $(n + 1)$s,p orbitals. In the square-planar complex the two ligands X and T share one p orbital located on the metal, but in the trigonal bipyramid the three equatorial ligands X, T, and Y share two p orbitals. Thus it is claimed that the p components of the M–X and M–T interaction are "firmed up" in the tbp intermediate, i.e., $^2/_3$ of a p orbital per ligand in the tbp and $^1/_2$ of a p orbital per ligand in the square plane (III). What,

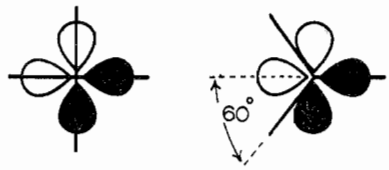

(III)

however, is neglected in this approach is the fact that whereas in the planar substrate the σ orbitals of X and T direcly overlap the lobes of (say) the metal p_y orbital, in the tbp such overlap is an indirect one (III). Correction for this geometrical factor using the angular overlap approach leads to the same "amount" of ligand $(n + 1)$p orbital interaction in both structures leading on this model to no firming up. In order to see this effect our model needs to be extended to energy terms containing[36] S^4.

As we noted above Vanquickenborne and co-workers[20,21] using the angular overlap approach have calculated the "ligand-field activation energy" for the profile of Figure 1a in a similar way to our derivation of Table II. However, there is one important difference. The LFAE calculated via this route is obtained in much the same way as the crystal-field activation energy is obtained on an earlier theory,[33] by requiring that the energy barycenter of the d orbital set remains constant in planar and trigonal-bipyramidal structures. Thus it is a mix of molecular-orbital and crystal-field ideas. It includes contributions from the π-bonding characteristics of the ligands which as we have seen above vanish for π donors with our method. We favor our present approach since it is a completely molecular orbital based model and does not assume arbitrary barycentering of the d orbitals.[34]

Derivation of Potential-Energy Surface

Table II shows that as the system moves from planar to tbp, the ligands of the planar system which occupy the axial sites of the tbp become more strongly bound and those which occupy the equatorial sites become less strongly bound. In support of this contention the hydrogen-isotope effect on the rates of reactions of *trans*-$Pt(PEt_3)_2HCl$ has been interpreted[35] in terms of a weakening of the Pt–T (in this case Pt–H) bond in the transition state. We are interested initially in the tbp intermediate (I) structure (Table II) where the entering trans and leaving groups are in the equatorial plane as in I. The intermediate tbp(II) will not result in loss of X or T via the process I. We describe the reaction coordinate in the following way by the parameter γ. For $\gamma = 0$ the angle $\alpha = 0°$ (IV)

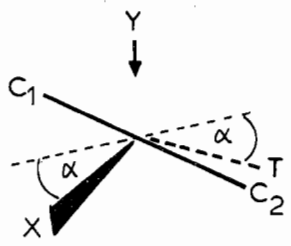

(IV)

and the entering ligand Y is not bound. This is the planar substrate alone. For $\gamma = 1$, $\alpha = 30°$ and the entering ligand has approached to its equilibrium bonded distance in the tbp intermediate. During this process we assume that all the ligands except the entering one have kept the same bond lengths. We may divide the energy changes involved into two different parts. First, the energy change contributed by the cis X and T ligands we allow to change smoothly as a linear function of γ. This is the energy change induced by the change in angular geometry only, as a response to the approach of the ligand Y. Second, the energy change contributed by the ligand σ–metal d orbital interaction of the incoming ligand contains a dependence upon the angular geometry of the complex and a contribution associated with the decrease in distance between metal and Y as the tbp structure is formed. We can readily appreciate this angular dependence. For the planar substrate, interaction of the fifth ligand to give a square-pyramidal molecule is zero on d orbital only grounds.[36] In the tbp, however, all ligands are bound. If we represent the distance dependence (arbitrarily) as $Y_\sigma(\gamma) = \gamma Y_\sigma$, i.e., a zero overlap integral at $\gamma = 0$ and a linear dependence on the angular geometry coordinate (we recall that this changes in response to the entering ligand approach), then the overall energetic behavior of the incoming ligand's d-orbital contribution to the total stabilization energy is a quadratic one, i.e., $^1/_2\gamma^2 Y_\sigma$. The total interaction energy of the metal with π-acceptor orbitals on the ligand Y is independent of geometry (since all metal–ligand bonding orbitals are filled) and is therefore included with a linear dependence on γ. A similar dependence for the same reason applies to ligand interactions with $(n + 1)$s,p metal orbitals. These results are summarized in Table III. The overall dependence of the stabilization energy on γ is then of the form

$$\Sigma = a - b\gamma + c\gamma^2 \tag{8}$$

where

$$\begin{aligned} a &= 3/2C_{1\sigma} + 3/2C_{2\sigma} + 3/2X_\sigma + 3/2T_\sigma \\ b &= X_\sigma + T_\sigma - 4Y_\pi - 1/2C_{1\sigma} - 1/2C_{2\sigma} - Y_\sigma \\ c &= 1/2Y_\sigma \end{aligned} \tag{9}$$

The minimum in $\sum$ occurs at $\gamma = a - b^2/4c$ and we sketch a typical curve in Figure 3 where we have the stabilization energies of substrate, bond-making transition state, and intermediate. By symmetry a similar curve represents also the energies of intermediate, product, and bond-breaking transition state. We emphasize that there is no real justification for the assumption that the d-orbital energy contribution associated with the entering Y ligand is dependent upon γ.[2] The use of the quadratic function here is beneficial in that it provides readily manageable algebraic functions to describe the barrier heights for bond making and bond breaking. We do not think

Table III. Energetic Dependence of Ligand Interaction on Geometry

	Angular change	Distance of entering ligand	Overall
$C_{1\sigma}, C_{2\sigma}, X_\sigma, T_\sigma$	Yes	No	γ
Y_σ	Yes	Yes	γ^2
Y_π	No	Yes	γ
Y_s	No	Yes	γ

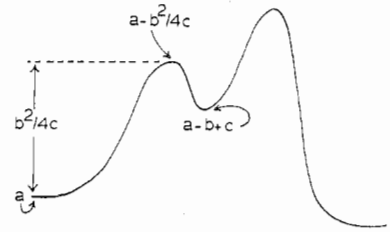

Figure 3. Parameters of the reaction potential surface. a, b, and c are defined in eq 9.

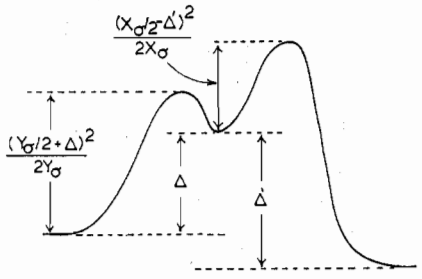

$\Delta = -C_{1\sigma}/2 - C_{2\sigma}/2 - Y_\sigma/2 + X_\sigma + T_\sigma - 4Y_\pi - Y_s$

$\Delta' = -C_{1\sigma}/2 - C_{2\sigma}/2 - X_\sigma/2 + Y_\sigma + T_\sigma - 4X_\pi - X_s$

Figure 4. Parameters of the reaction potential surface in terms of the tbp–sp energy differences, Δ, Δ'.

that derivation of a more "realistic" dependence would be a particularly useful exercise with a model which, although simple, is also rather crude.

Two points of interest present themselves immediately. First, if $b < 0$ then there is no barrier between planar substrate (or product) and tbp intermediate. Second, for the barrier to occur between $0 < \gamma < 1$ (i.e., a physically meaningful situation) $b < 2c$. This is quite a restriction on d-orbital grounds alone with π-donor ligands but if the ligand interaction energy with the $(n + 1)$s,p orbitals of the metal is included then this requirement is almost certainly taken care of.

A particularly useful way of viewing these energy parameters is to express the energy differences as a function of Δ, the stabilization energy difference between planar and tbp structures. Figure 4 shows the result. Below we shall make use of both Figures 3 and 4 to relate the observed kinetic behavior to this energy surface.

Features of the Substitution Process. Dependence on Entering and Leaving Barriers

From the limited number of cases where data are available it is clear[1] that within a related series of reactions an increase in reaction rate is associated with a decrease in activation energy. Thus we are looking at the right factor (potential-energy surface) in trying to rationalize relative rates of chemical reaction. However, the overall rate of reaction is in general a complex function of the two barrier heights of Figure 1b: one for bond making and one for bond breaking. It depends upon whether the intermediate is in equilibrium with the starting material or can be treated as a transient destroyed very rapidly after formation to give products.[37] There is no evidence from the form of the rate law for accumulation of intermediate in the overwhelming majority of systems studied. We shall therefore use the simple scheme V. Applying stationary-state conditions to the intermediate

$$\text{substrate} \underset{k_1'}{\overset{k_1}{\rightleftharpoons}} \text{intermediate} \begin{cases} \xrightarrow{k_2} \text{product a} \\ \xrightarrow{k_3} \text{product b} \end{cases} \qquad \text{(V)}$$

the overall reaction rate constant for production of a is $k_1'k_2/(k_1 + k_2 + k_3)$. In a large number of cases the tbp intermediate will be less stable than substrate or product in which case $\Delta E_1, \Delta E_2, \Delta E_3 \ll \Delta E_1'$ and the rate-determining barrier is the bond-making one. Assuming equal pre-exponential terms then $-\log k \sim \Delta E_1'/RT$ is determined by the entering barrier. If the tbp intermediate is more stable than the substrate then the entering barrier may well be very small (or nonexistent) and the rate then becomes determined by the bond-breaking barrier. To gain a clue as to which alternative arises we need to put in some numbers for values of the σ, π parameters of the model from Table I but even then, although we have quantitative values for the $\beta_\sigma S_\sigma^2$ parameters, we have no quantitative feel for the relative magnitudes of ligand interactions with the higher energy $(n + 1)$s,p orbitals. We defer the numerical approach until we have looked at the algebraic form of the potential function in a general effort to glean some information about the process in general. With any comments concerning rates of reaction the reader should therefore bear in mind the fact that in all instances the barrier height or combination of barrier heights determining the rate is not an experimentally observed fact.

Cattalini and co-workers[38] decided that the leaving barrier was higher than the entering one from studies of the rates of displacement of thioethers from $Pt(bpy)ClR'SR^+$. Here the reaction rates were markedly dependent upon the nature of R and R', i.e., upon the nature of the leaving group. However, we must be careful in drawing such conclusions from this observation since in reaching the *entering* transition state we have weakened (partially "broken") both the M–X and M–T bonds. The larger M–X bond-breaking contribution however does most certainly come as the system passes over the second transition state to product.

Dependence on Entering Barrier

(a) Systems with π-Donor Ligands. We initially consider π-donor systems alone and ignore interactions with the $(n + 1)$s,p orbitals on the central metal atom. For the barrier due to the bond-making transition state we see from Table II or Figure 4 that the σ-donor strength of all the ligands appears but that the only π contribution is in that case where the entering ligand is a π acceptor. One series we shall find essential in our discussion is the quantitative ordering (Table I) of σ-donor strength (albeit derived for the Cr^{III} system) from the recent work of Schäffer and co-workers.[29] The order is

$$OH^- > H_2O > F^- > NH_3 > py > Cl^- > Br^- \qquad (10)$$

The actual values of $\beta_\sigma S_\sigma^2$ are expected to increase down the periodic table just as Δ_{oct}, the t_{2g}/e_g^* separation in octahedral complexes, changes. Thus any barriers should be larger for Pt^{II} than for Pd^{II} which in turn should be larger than for Ni^{II}. As a rough guide the relative reaction rates are found in the ratios $Pt^{II}:Pd^{II}:Ni^{II} = 1:10^5:10^7$.

If all the ligands are identical (isotopic exchange) and π donors then the tbp structure becomes a transition state as substitution into the equations of Figure 3 shows. The barrier height for exchange of X is equal to Δ the tbp/planar energy separation. This activation energy is then simply $^1/_2X_\sigma$ and the rates of reaction 11 where X = halide are expected to

$$PtX_4^{2-} + X^{-*} \rightarrow PtX^*X_3^{2-} + X^- \qquad (11)$$

decrease as the σ-donor strength increases. With reference to sequence 10 we expect the rates therefore to go as $I^- > Br^- > Cl^-$ which indeed is the experimentally observed order.[39]

The expression for the entering barrier height (eq 12) in-

entering barrier height =

$$\frac{(X_\sigma + T_\sigma - {}^1/_2C_{1\sigma} - {}^1/_2C_{2\sigma} - 4Y_\pi - Y_\sigma)^2}{2Y_\sigma} \qquad (12)$$

dicates that on d-orbital σ grounds alone the rate should behave in the opposite direction when a particular ligand is the entering one (appears in the denominator) compared to when it is present as X or T in the complex (appears in the numerator). There are however few systematic studies available in this field to check this suggestion but correspondence with theory is found in a series of observations on some Au, Pt, and Pd amine systems. For reaction 13, as the pK_a of the entering

$$Pt(bpy)Cl_2 + am \rightarrow Pt(bpy)Cl(am)^+ + Cl^- \qquad (13)$$

amine increases (increasing pK_a probably represents a stronger

Table IV. Some n_{Pt}^0 Values

Cl^-	3.04	Br^-	3.96	Ph_3Sb	6.79
py	3.13	I^-	5.42	CN^-	7.14
NO_2^-	3.22	SCN^-	5.65	Ph_3P	8.93

σ donor and thus larger value of $\beta_\sigma S_\sigma^2$) the barrier height decreases and the reaction rate increases.[40] However, with the series of reactions 14 increasing the pK_a of the amine in

$$trans\text{-}Pd(am)_2Cl_2 + RSR' \rightarrow trans\text{-}Pd(am)RSR'Cl_2 + am \quad (14)$$

the complex leads to a decrease in reaction rate.[41] Similar results are found[42] for reaction 15 depending upon whether

$$PtCl(DMSO)^- + am \rightleftharpoons trans\text{-}PtCl_2(am)(DMSO) + Cl^- \quad (15)$$

the amine is the entering group or present initially in the complex. Such gratifying accord with eq 12 is however not universal in these amine studies. Some other systematic studies varying the amine present in the system often give the opposite result to that expected on the basis of this equation[43,44]

(b) Inclusion of Higher Energy Orbitals and π Acceptors. Increasing barrier height with decreasing $\beta_\sigma S_\sigma^2$ of the entering ligand as predicted by Figure 3 is not found in general and is a limitation of the descriptive power of the d orbital only model. The values of n^0_{Pt} for different ligands, a measure of the relative rates of attack on a standard substrate, are given for a few ligands of interest in Table IV. $I^- > Br^- > Cl^-$, whereas on the basis of the σ-donor order of (10) and the d-orbital only model the order should be reversed. However, the size of the interactions of the ligand with the $(n + 1)$s and $(n + 1)$p orbitals and whether the ligand can function as a π acceptor will also determine the size of the entering barrier. We see from Figure 4 why these considerations are very important. The π-acceptor strength is weighted four times as heavily as the σ strength of the X or T ligands and twice as heavily as the σ strength of the entering ligand. Thus, whereas ligand π strengths are generally thought of as being typically 20–30% as large as the corresponding ligand σ strengths, this factor means that π-acceptor properties may be easily twice as important as the σ properties of the entering ligand in determining the barrier height.

With reference to the isotopic exchange reactions 11, exchange of CN^- occurs faster[39] than for any of the halide ions. CN^- is certainly a better σ donor than I^- which should result in rate (CN^-) < rate (I^-) on σ grounds alone. In addition, however, the ligand is a good π acceptor and is able to stabilize the transition state. For the related Ni^{II} system the stable species $Ni(CN)_5^{3-}$ has been isolated and characterized by x-ray crystallography.[45] We have commented on this particular stabilization effect by π acceptors before.[36]

Similar importance is attached to the higher orbital interactions between ligand and metal. Large stabilization energies from this source (large Y_σ) reduce the barrier in a similar way to a large π acceptor strength (Y_π). Thus good π acceptors and ligands with good interaction with $(n + 1)$s,p orbitals on the metal will be those ligands with high n_{Pt}^0 values. In summary (the arrow indicates the direction of increasing n_{Pt}^0)

$$\text{increasing } \pi\text{-acceptor nature of entering ligand} \longrightarrow \quad \text{(VIa)}$$

$$\text{increasing interaction with } (n + 1)\text{s,p orbitals} \longrightarrow \quad \text{(VIb)}$$

$$\text{increasing d-orbital interaction} \longrightarrow \quad \text{(VIc)}$$

From calculated values[15] of VIb, this order is in the opposite direction for most ligands than is the $\beta_\sigma S_\sigma^2$ order, VIc. I.e, $\beta_\sigma S_\sigma^2$ for the halide ions is in the order $F^- > Cl^- > Br^- > I^-$ but the best interaction with higher energy orbitals is for I^- and the poorest for F^-. Examination of the n_{Pt}^0 values of Table III leads to the conclusion that it is VIa and VIb which largely determine these values as suggested by the relative contributions of Y_σ, Y_π, and Y_s to the barrier height in Figure 4. However, in some circumstances where Y_π and Y_s are likely to be constant (ligands containing the same donor atom for instance) then smaller variations in Y_σ will appear to determine the reaction rates as we noted above in the systematic amine studies.

It is instructive to couch some of the language of the existing literature in this field in these molecular orbital terms. It has been pointed out by several authors that the basicity of the incoming ligand plays only a minor role in determining the reactivity (n_{Pt}^0 values) as we noted above. (Thus strongly basic ligands such as OH^- and CH_3O^-, for example, do not react well with Pt^{II} substrates, since $Y_s \sim 0$ and $Y_\pi = 0$ even though Y_σ may be quite large.) The most important factor is claimed to be the "softness" or micropolarizability of the entering ligand. This concept[46] results "from the existence of low-lying states which when mixed with the ground state produce polarity". In molecular orbital terms this mixing in of excited states of the individual fragments has been examined theoretically[15] and used to rationalize the geometries of coordinated ligands. In symmetry terms Mingos[47] has used the pseudo-Jahn–Teller formalism to examine the same effect. Soft ligands are those with low-lying π-acceptor levels and also ligands such as I^-, Br^-, etc. F^-, H_2O, and OH^-, ligands with good σ-donor power but poor interaction with metal $(n + 1)$s,p orbitals, are hard ligands. Thus the micropolarizability order of the n_{Pt}^0 series in the reactions at Pt^{II} centers mirrors the interplay of the three terms Y_σ, Y_π, and Y_s according to Figure 4.

(c) Dependence upon the Nature of the Ligands X, T. The dependence of entering barrier on the nature of the replaceable ligand X and the trans ligand T should be a much simpler one from eq 12. From Figure 4 increasing the σ strength of either ligand results in an increase in barrier height. Thus increasing the σ donor power (measured by the Taft σ^* parameter) of a coordinated phosphine in a square-planar substrate leads to a reduction in rate constant.[48] Therefore as X is varied the reaction rate increases as the σ-donor strength of X decreases. The effect is quite marked and means that there is partial M–X "bond breaking" on forming the transition state as we have discussed above. Thus for ejection of the ligand X from the planar substrate the rate decreases in the order of sequence 10, i.e., rate (X = iodide) > rate ($X = H_2O$). Experimentally for a series of reactions it is generally observed that the order of lability is $I^- > Br^- > Cl^-$ in agreement with this.[49-51] Similarly as the pK_a of the leaving amine increases in reaction 15 the slower the reaction proceeds. This effect is also reproduced with similar studies[43] on Cl^- substitution of an amine in $cis\text{-}Pt(am)_2(DMSO)Cl^+$.

By symmetry in X and T this order is also that of the trans labilizing effect and for π-donor ligands the correspondence between the order of the two sequences 3 and 10 is very pleasing. Since the incoming barrier from Figure 4 is given by $(\Delta + {}^1/_2Y_\sigma)^2/2Y_\sigma$ then arguments about the trans labilizing order using the profile of Figure 1a and values of Δ alone will give the same order as we generated here for constant incoming ligand Y. However, whereas the Figure 1a profile gives the correct qualitative dependence of rate on X and T ligands it is unable to treat the much more complex dependence on entering ligand.

A very interesting feature of this treatment is that the trans labilizing order is independent of the π-acceptor properties of the ligand T. There is not in fact very much experimental data concerning this point. One set of results[1] on system 16 shows that the rate decreases in the order $C_2H_4 \gg NO_2 > Br^- > Cl^-$ = T. The usual explanation of this order is the high π-acceptor

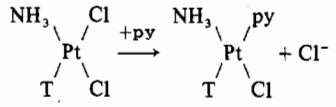

(16)

power of ethylene which our theory tells us is not of importance. However, we do not have a quantitative feel for how strong a σ donor the C_2H_4 ligand is. Qualitatively it may be a poor σ donor and if worse than NO_2 we have a more valid rationalization of the position of ethylene in the sequence describing the rate of reaction 16. This is certainly an area where further kinetic studies are needed.

Role of the Cis Ligands

We may get some idea as to the relative importance of the cis ligands from the tbp–substrate energy difference Δ (eq 17).

$$\Delta = X_\sigma + T_\sigma - {}^1/_2C_{1\sigma} - {}^1/_2C_{2\sigma} - Y_\sigma - 4Y_\pi - Y_s \qquad (17)$$

The effect of variations in the nature of the cis ligands is half as sensitive to changes in the trans ligand. (This will be reproduced also in the size of the entering barrier where Δ appears as a squared term.) The effect is, in addition, in the opposite direction. In general, the cis effect should then be smaller than the trans effect. Also if the σ-donor strengths of the ligands X and T dominate Δ then the cis effect could be expected to be quite small indeed. The cis effect seems in practice to be a very variable phenomenon and present experimental evidence does not allow any definite universal trends to be identified. However, anticipating our quantitative discussion below we find that the conclusions drawn from theory in this section are well matched by systematic experimental observations when Cl^-, H_2O, NH_3, or DMSO are ligands but it is much more difficult to accommodate the reasonably large amount of much more fragmentary evidence concerning perhaps single observations on systems containing other ligands.

General Form of the Rate Constant

The rate of reaction (k_Y) of a ligand Y with a substrate is often represented[52] by the approximate relationship (18) where

$$\log k_Y = sn_{Pt}{}^0(Y) + \log k_s \qquad (18)$$

k_s is the rate constant for attack of solvent (independent of Y of course) and s, the discrimination, has a value dependent on the nature of the substrate and independent of the nature of the entering ligand. $n_{Pt}{}^0(Y)$ as we noted above is a measure of the rate of attack of Y on a standard substrate, relative to the attack of solvent on the substrate. It is dependent therefore only on the nature of Y. This equation fits the observed rate constants in a reasonably rough and ready fashion. If the entering barrier alone determines the rate of reaction then we find eq 19 by manipulation of eq 12 where q is a term con-

$$\log k_Y = sn_{Pt}{}^0(Y) + \log k_s + q \qquad (19)$$

taining dependence on both the nature of the substrate and entering ligand. If we assume that the activation barrier to the reaction is given by Δ of Figure 4 (i.e., a profile of the form Figure 1a) then eq 20 results. Here $\log k_Y/k_s$ is substrate

$$\log k_Y = n_{Pt}{}^0(Y) + \log k_s \qquad (20)$$

independent ($s = 1$ always). This is clearly not the case and is additional evidence against the Figure 1a profile. If q is small however then the observed kinetic eq 18 can be matched to our model, especially since this equation does not fit the experimental data all that accurately. The deviations from eq 18 observed for poor σ donors (e.g., thiourea) as entering ligands which are found experimentally[52] may be associated with the fact that the leaving barrier now determines the rate as we suggest below. The height of the entering barrier then gives a good qualitative measure of the reaction rates in these systems including the special case of the trans-labilizing effect. In order to see which ligand is ejected from the intermediate we need however to look at the factors affecting the size of the leaving barrier.

Leaving Barrier

The barrier for loss of ligand (Figure 4) X is simply given by $({}^1/_2X_\sigma - \Delta)^2/2X_\sigma$ where Δ is the energy difference between tbp intermediate with X and the planar product without X. X_σ is the σ-donor strength of the leaving ligand. Two cases emerge: (a) if $\Delta < {}^1/_2X_\sigma$ then the larger the Δ the smaller the leaving barrier; and (b) if $\Delta > {}^1/_2X_\sigma$ then the smaller the Δ the smaller the leaving barrier. Case (a) is generally expected to be the case in the majority of systems and especially so with ligands which have good involvement with $(n + 1)$s,p orbitals or are π acids or poor σ donors. The ligands which stabilize the tbp relative to square-planar substrate (reduce Δ) are those of poor σ donor power. Thus the smallest leaving barrier is expected to arise for good σ donors. For π-donor systems therefore the stronger σ donor (out of X or T) should be ejected. Vitally gratifying is that the trans-effect order (trans-directing order) of sequence 3 is the same as that of sequence 10; i.e., the best trans directors are the poorest σ donors. Previous rationalizations[16,17] of this order have used the hypothesis that the bond most weakened on moving to the transition state of Figure 1a is the one that is broken. From Table II we see that it will be the stronger σ donor of X or T which experiences the larger loss in stabilization energy. Thus use of this hypothesis gives the correct answer when applied to the crude profile of Figure 1a. Ligands which have small values of Δ include those where interaction with $(n + 1)$s,p orbitals on the central atom is large or where π-acceptor orbitals are present. These ligands will experience large barriers for their loss and be good trans directors. Thus good trans directors are so by virtue of the fact that they are reluctant leaving groups rather than any inherent directing property. Because of the symmetry in Δ in Figure 4 between entering and leaving barriers we would also expect to find that the trans-labilizing series was approximately the reverse of the $n_{Pt}{}^0$ series and in several respects this is true. High values of $n_{Pt}{}^0$ (CN^-, phosphines) give high barriers and poor loss of this ligand (good trans directors) whereas small values of $n_{Pt}{}^0$ give low barriers and ready loss of this ligand (poor trans directors). We may therefore summarize (the arrow indicates the direction of the trans-direction effect)

increasing interaction with $(n + 1)$s,p orbitals ← (VIIa)

increasing π-acceptor character ← (VIIb)

increasing σ-donor strength → (VIIc)

~increasing $n_{Pt}{}^0$ ← (VIId)

For the series $n_{Pt}{}^0$ itself we concluded that effects VIIa and VIIb outweighed VIIc. However, in this case the effects VIIa and VIIc reinforce each other whereas for the $n_{Pt}{}^0$ series VI they were opposed. Thus some differences between the $n_{Pt}{}^0$ series and the trans-effect series may be expected. As with the $n_{Pt}{}^0$ series the heavy weighting of the π-acceptor character of the leaving ligand in the leaving barrier seems to dominate the series. For the hydride ligand where π-acceptor properties are absent its high trans-directing ability is ascribed to very large interaction between the hydrogen 1s orbital and the $(n + 1)$s,p orbitals on the metal. This is clearly indicated by quantitative molecular-orbital calculations.[15-17] Perhaps however we should exercise some caution with this ligand. The presence of the hydride ligand in transition-metal complexes usually leads to distorted structures[53] (we have assumed an

ideal trigonal bipyramid in our deliberations) which may be reached by a lower energy pathway from starting materials (high trans-labilizing effect) and from products (high trans-directing influence) than the route used here.

Apparent Exceptions to the Trans-Effect Order

Which of the two possible tbp structures VIII is ap-

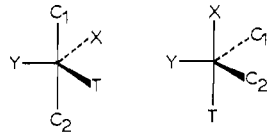

(VIII)

proachable via the lower energy barrier, i.e., which of the two pairs of ligands are most likely to end up in the equatorial plane? A comparison of the two stabilization energy differences (Table II) tells us that the stronger σ donors go into the axial positions of the trigonal[54] bipyramid to give the lower energy structure and barrier. With reference to our discussion above therefore the ligand displaced from the planar molecule is the stronger field ligand along the weaker field axis of the planar substrate. This seems to be a useful rule, at least for systems containing π donors alone. Stated this way it has some striking resemblances to Adamson's rules in Cr^{III} photochemistry[56] where a ligand is ejected from an electronically excited molecule.

Some apparent exceptions to the trans-effect order may be rationalized by consideration of the energies of the two possible tbp molecules. For example Cl^- is always displaced[57] in reaction 21, where Y = Cl^-, Br^-, I^-, SCN^-, and tu, in spite of

$$trans\text{-}Pt[(PEt_3)(pip)Cl_2] + Y^- \rightarrow trans\text{-}[PtPEt_3(pip)ClY] + Cl^- \quad (21)$$

the high position of the phosphine in sequence 3. Loss of pip would imply a tbp intermediate with the two Cl^- groups occupying axial positions and loss of Cl^- would imply an intermediate where PEt_3 and pip occupied these sites. Which axis is labilized depends therefore on the relative σ-donor strengths of the ligands and not on the relative positions in the trans-effect order. While these are the same for π donors they are different for π acceptors. The result of eq 21 could then be rationalized if the average σ-donor strength of PEt_3 and pip was greater than that of Cl^-.[58]

If the Leaving Barrier Determines the Rate

We have assumed above that the entering barrier controls the rate of reaction, but in what circumstances would the entering barrier be depressed and the height of the leaving barrier control the rate? It will depend upon the nature of the incoming ligand, Figure 5. If the incoming ligand is a poor σ donor or a good π acceptor or has good interaction with $(n + 1)$s,p orbitals on the metal then Δ may be small or even negative such that the entering barrier is small or nonexistent (Figure 5b). For entering ligands with the opposite properties the height of the entering barrier will govern the rate (Figure 5a). Whereas the entering barrier is proportional to the function $(\Delta + {}^1/_2Y_\sigma)^2$, the leaving barrier height is $({}^1/_2X_\sigma - \Delta')^2$. Thus our conclusions above concerning the trans and cis ligand effects on the reaction rate are reversed if the leaving barrier is rate determining.

A reversal of trans-effect order has indeed been observed when poor σ donors (soft bases) such as thiourea and iodide are used as entering ligands. (The trans-effect order quoted in (3) is the one generated with pyridine as incoming ligand. This is a good donor and hard base (Table I).) Thus, for example, with the series of reactions 22 the rate depends[13]

$$trans\text{-}Pt(Et_3)_2TCl + Y^- \rightarrow trans\text{-}Pt(PEt_3)_2TY + Cl^- \quad (22)$$

markedly on the nature of T, but the sequence T = CH_3 > C_6H_5 > Cl is obtained for NO_2^-, Br^-, and N_3^- as entering ligands and the order CH_3 > Cl > C_6H_5 when the soft ligands

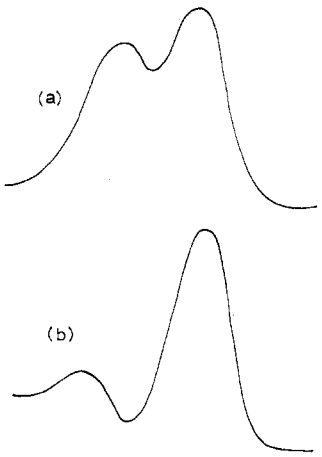

Figure 5. Schematic representations of two extreme behavioral types: (a) entering ligand does not heavily stabilize the tbp intermediate; (b) entering ligand dramatically stabilizes the tbp intermediate.

I^- and thiourea are entering groups.

Reversal of the cis effect as a function of entering ligand has also been observed experimentally. If we assume that py is a better σ donor than PEt_3 then for good σ donors as entering ligands for reaction 23 the rate is determined by the entering

$$trans\text{-}PtL_2Cl_2 + Y^- \rightarrow trans\text{-}PtL_2ClY + Cl^- \quad (23)$$

barrier and the rate (L = PEt_3) < rate (L = py). For[59] Cl^- as entering ligand rate (PEt_3) = 2.9×10^{-5} M^{-1} s^{-1} and rate (py) = 4.5×10^{-4} M^{-1} s^{-1}. For a poor σ ligand as entering group then the rate is determined by the leaving barrier and we predict rate (L = PEt_3) > rate (L = py). For I^- as entering ligand the reverse behavior is observed; rate (PEt_3) = 0.236 M^{-1} s^{-1} and rate (py) = 0.107 M^{-1} s^{-1}. This particular result has been interpreted[5] in a qualitative way in terms of distribution of charge of the incoming nucleophile via π bonding, but from Figure 2 the π-bonding capabilities of the other ligands do not enter into consideration. Such evidence obviously is not conclusive proof of a leaving barrier determined reaction but it is certainly in the direction expected when soft ligands (poor σ donors) are used as entering groups.

Some Examples Treated Numerically

We have seen that the interaction of the incoming ligand with higher energy $(n + 1)$s,p orbitals on the central atom contributes vitally to the incoming barrier height for ligand substitution. However, we are limited in quantitative manipulations of the equations of Figure 4 because although the figures for d-orbital interaction are available for some ligands (Table I) data for the sizes of the interaction with $(n + 1)$s,p orbitals are not. In order to minimize this problem we consider numerically systems which are related by having the same incoming ligand in order to test out the d-orbital part of the model. Thus calculated barrier heights (if they have any absolute meaning at all since we are using Cr^{III} parameters in a Pt^{II} system) are not transferrable between systems containing different entering ligands. For the same reason there is no point in comparing calculated barrier heights with those experimentally deduced.

There is only one series of relatively complete studies available in the literature and that is for the hydrolysis, ammoniolysis, and anation reactions of the species $Pt(H_2O)_x(NH_3)_yCl_{4-x-y}$. Less complete data are available for their Br^- and Pd analogues. Coe's review[7] collects together all the available data on these systems in a very useful tabular fashion. We focus attention on different sets of reactions in this area and use our theory to calculate barrier heights for each reaction. In part we adopt this strategy because different groups of workers often use different experimental conditions

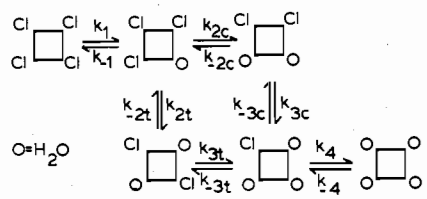

Figure 6. Substitution reactions of a square-planar ML_4 complex.

Table V. Rate Constants and Calculated Barrier Heights for the Hydrolysis and Anation Reactions of $Pt(H_2O)_xCl_{4-x}$

	Calcd entering barrier, μm^{-1}	Calcd leaving barrier, μm^{-1}	Δ, μm^{-1}
k_1[a]	0.195	0.050	0.159
k_{2c}	0.121	0.013	0.042
k_{2t}	0.395	0.20	0.395
k_{3t}	0.064	0	−0.076
k_{3c}	0.286	0.113	0.277
k_4	0.195	0.050	0.159
k_{-1}	0.563	0.035	0.513
k_{-2c}	0.408	0.079	0.395
k_{-2t}	0.949	0	0.749
k_{-3t}	0.277	0.14	0.277
k_{-3c}	0.743	0.009	0.631
k_{-4}	0.563	0.035	0.513

[a] Rate constants defined in Figure 6.

of temperature and ionic strength and sometimes solvent.

Aquation of PtX_4^{2-} and Halation of $Pt(H_2O)_4^{2+}$ (X = Cl, Br)

The rates of successive aquation of $PtCl_4^{-2}$ have been extensively studied and all six rate constants have been determined (Figure 6). The most complete data are those of Elding.[60-62] For the reverse reactions, incorporation of Cl^- into $Pt(H_2O)_4^{2+}$, all six rate constants have been evaluated. Less complete data are available for the analagous bromide case.[63,64] For the Pd system the rate constants are about 10^5 larger.[65] One striking feature of these rate constants is that their relative ordering seems to be the same in all the examples studied (eq 24). (The parentheses indicate two rate constants which are

$$k_{3t} > k_{2c} > k_1 > (k_4) > k_{3c} > k_{2t}$$
$$k_{-3t} > k_{-2c} > (k_{-4}) > k_{-1} > k_{-3c} > k_{-2t} \quad (24)$$

not well determined.) Vrankx and Vanquickenborne showed[21] that this order could be achieved if the LFAE was calculated for the difference in barycentered energy between tbp and planar substrate. Here we use the molecular-orbital stabilization-energy differences for planar substrate, tbp intermediate, and the two transition states associated with the reaction profile. Table V gives for the 12 reactions of Figure 6 describing reaction 25 values calculated for the incoming

$$PtCl_x(H_2O)_{4-x} + H_2O \rightarrow PtCl_{x-1}(H_2O)_{5-x}$$
$$PtCl_x(H_2O)_{4-x} + Cl^- \rightarrow PtCl_{x+1}(H_2O)_{3-x} \quad (25)$$

and leaving barriers as well as the molecular-orbital energy differences between planar substrate and tbp intermediate. With d orbitals alone it is the bond-making process which determines the reaction rate. The same relative ordering of rate is predicted using (a) entering barrier alone, (b) the sum of the entering + leaving barriers, and (c) the planar–tbp energy separation Δ. In two cases there is no barrier to bond breaking which means that the bond making transition state is overall the transition state for the reaction. (This however is on the d orbital only scheme). For one case Δ is negative, giving rise to a negative activation energy if the profile of Figure 1a is used.

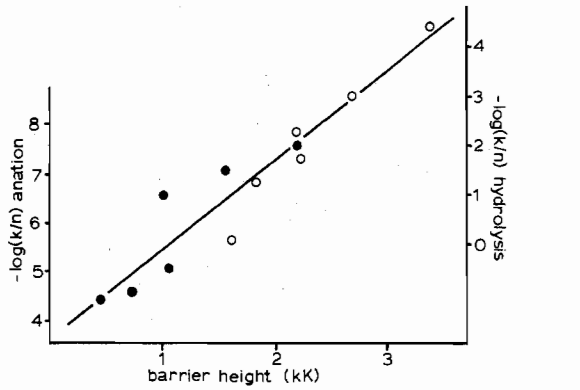

Figure 7. Calculated values of the sum of entering and leaving barrier heights for the hydrolysis and anation of $PtCl_x(H_2O)_{4-x}$. The origin of the scale describing the reverse reaction has been moved such that the full circles (forward reaction) and open circles (reverse reaction) lie on the same straight line.

The trans-effect order suggests that $k_{3c} > k_{3t}$ and $k_{-2t} > k_{-2c}$ since $Cl^- > H_2O$ which is also the order found numerically. Here is a case of the labilization of the stronger σ donor ($Cl^- < H_2O$) along the weaker field axis as we noted above. Figure 7 gives a plot of log k/n against the sum of entering and leaving barriers of Table V (n is the number of equivalent replaceable ligands). The agreement is quite convincing. A not quite such good fit is obtained if Δ values are used instead.

Several other results are explicable on similar grounds. The ordering of rate constants for reaction of NH_3 with $PtCl_x(NH_3)_{4-x}$ determined by Martin[66] is the same as for the above and the plot (not shown) of calculated barrier height against log (k/n) gives a straight line fit as good as Figure 7. The results of Rheinhardt and co-workers[67,68] on the rates of NH_3 replacement in $PdCl_x(NH_3)_{4-x}$ also fit into the scheme. A similar plot of calculated barrier height against log (k/n) shows a good correlation between the two. This particular ordering of rate constants (eq 24) for the MA_4/B exchange reactions seems then to be quite a general one and one which is well matched by our theory. The particular ordering of the rate constants depends only on which (of A or B) is the stronger σ donor.

Acid Hydrolysis of $PtCl_x(NH_3)_{4-x}$

Martin and co-workers have, in a series of papers,[69-74] extensively examined the acid hydrolysis rates of these mixed chloroammines (reaction 26). In some cases the rate constants

$$Pt(NH_3)_xCl_{4-x} \xrightarrow{+H_2O} Pt(NH_3)_xCl_{3-x}H_2O + Cl^- \quad (26)$$

for secondary hydrolysis were obtained (reaction 27). This

$$Pt(NH_3)_xCl_{3-x}H_2O + H_2O \rightarrow Pt(NH_3)_xCl_{2-x}(H_2O)_2 + Cl^- \quad (27)$$

is a more complex example than the previous one since it contains three different ligands. Table VI gives the rate constants at 25 °C for both primary and secondary hydrolyses and the calculated sum of entering and leaving barriers. In Figure 8 we plot these log k/n values against the barrier height and the agreement is excellent for all the systems except for H_2O attack on $PtCl_4^{2-}$ itself. The good fit for the value for primary hydrolysis of *cis*-$Pt(NH_3)_2Cl_2$ leads us to accept Martin's figure for this rate constant rather than a higher one obtained by Bannerjea et al.[75] The rate constants were found[74] to fit within 20% eq 28, where m is the number of NH_3 ligands

$$k/n = 1 \times 10^{-5}(0.5)^m(2.4)^p \quad (28)$$

trans to the replaced Cl^- (0 or 1) and p is the number of NH_3 ligands cis to the replaced Cl^- (0, 1, 2). There is no obvious dependence of rate constant on the charge on the complex from

Table VI. Rate Constants and Calculated Barrier Heights for $PtCl_x(NH_3)_{4-x}$ Hydrolyses at 25 °C

System	Calcd entering barrier height, μm^{-1}	Calcd leaving barrier height, μm^{-1}	Obsd rate constants, $s^{-1} \times 10^5$
Primary hydrolysis			
$PtCl_4^{2-}$	0.194	0.050	0.39
$Pt(NH_3)Cl_3^-$ (trans)	0.313	0.133	0.06
$Pt(NH_3)Cl_3^-$ (cis)	0.156	0.024	0.56
cis-$Pt(NH_3)_2Cl_2$	0.250	0.087	0.25
trans-$Pt(NH_3)_2Cl_2$	0.104	0.007	0.98
$Pt(NH_3)_3Cl$	0.194	0.050	0.26
Secondary hydrolysis			
$PtCl_4^{2-}$	0.121	0.013	0.33
$Pt(NH_3)Cl_3^-$			
k_t[a]	0.313	0.133	0.040
k_c	0.145	0.024	0.306
k_{ct}[c]	0.217	0.064	0.59
k_{cc}[c]	0.324	0.142	0.28[d]
k_{tc}[c]	0.083	0.002	0.72
k_{-t}[b]	0.795	0.005	3.055
k_{-c}[b]	0.462	0.061	2.690
cis-$Pt(NH_3)_2Cl_2$	0.165	0.033	0.33
trans-$Pt(NH_3)_2Cl_2$	0.260	0.094	0.5

[a] See Figure 9 for definition of symbols. [b] Recombination reactions, units $M^{-1}\ s^{-1}$. [c] At 20 °C. [d] Uncertain value.

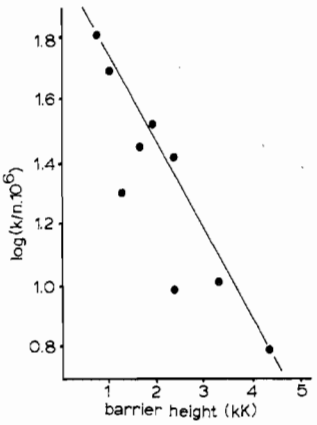

Figure 8. Calculated barrier height vs. observed log (statistical rate constant) for the primary (I) and secondary (II) hydrolysis reactions of $Pt(NH_3)_xCl_{4-x}$ species. Experimental values for 25 °C. (10 kK = 1.0 μm^{-1}.)

Figure 8 indicating perhaps that it is the associative step which is rate determining (neutral + charged or neutral species) rather than the dissociative one (charged + charged or neutral species) in agreement with the fact that our calculated entering barrier is larger than the leaving one. The apparent charge dependence observed by Martin et al.[74] is simply a consequence of the stepwise replacement of Cl^- by H_2O. A similar dependence on the number and type of ligands present would be expected on the present scheme by replacement of one ligand by another irrespective of whether the charge on the complex changed or not.

Figure 9 shows the scheme for the primary and secondary hydrolyses of the $PtCl_3NH_3$ complex.[74] The rate constants k_{cc}, k_{ct}, etc., and their calculated barriers are plotted in Figure 10. k_{cc} is not well determined by the experimental data and by extrapolation a more reasonable value is $3 \times 10^{-6}\ s^{-1}$ rather than the value of about 2.8×10^{-5} given by Martin and co-workers. This may well be one useful practical feature of our method, fixing more accurately ill-defined reaction constants. k_{ct} also does not fit very well on this graph. An estimate better in line with the others would be around $1 \times 10^{-6}\ s^{-1}$. There

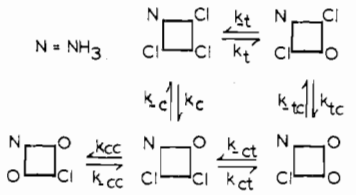

Figure 9. Reaction scheme for first and second hydrolyses of $Pt(NH_3)Cl_3^-$.

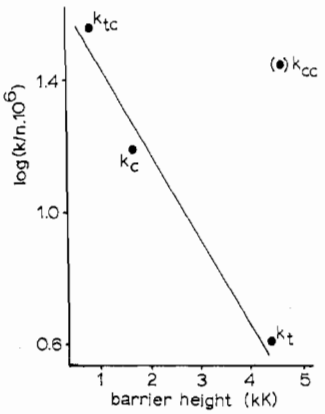

Figure 10. Primary and secondary hydrolysis rate constants for $Pt(NH_3)Cl_3^-$ vs. calculated barrier height. Experimental values for 20 °C.

is no evidence to suggest that this point contains any large experimental uncertainty, however.

The agreement between theory and experiment is good (Figure 8) with the exception of the data for $PtCl_4^{2-}$ itself. (The results of Martin and co-workers and those of Elding on this system are substantially the same.) Use of the entering barrier alone in such a plot gives a satisfactory fit again with these values not so obviously off course. A general feature of this plot is that it is steeper. This is the result of the general observation that the height of the leaving barrier increases with increasing height of the entering barrier. The two reverse rate constants k_{-c} and k_{-t} for the acid hydrolysis of $PtNH_3Cl_3$ are also in the correct order with regard to the sizes of the relevant barrier sum. However, since they arise via a different entering ligand to the above they cannot be plotted usefully on the same graph as Figure 8.

We return now to a discussion of eq 28. Because of the relative sizes of the two exponential parameters Martin and co-workers concluded[75] that "the cis neighbor has somewhat a greater influence on the kinetics than the trans neighbor". This arises from eq 28 since $1/0.5 < 2.4$. A least-squares refinement gives us a similar result (eq 29). However, from

$$k/n = 1.108 \times 10^{-5}(0.5321)^m(2.138)^p \quad (29)$$

Figure 8 the result for $PtCl_4^{2-}$ may well be anomalously small for reasons which are not clear at present. A least-squares refinement of the remaining data gives an answer (eq 30)

$$k/n = 1.325 \times 10^{-5}(0.4804)^m(1.982)^p \quad (30)$$

contrary to that represented by eq 28 and 29 with an rms deviation half as large as that for eq 29, with the $PtCl_4^{2-}$ point eight standard deviations away from this new line. This is a statistically better fit. Here the susceptibility to the nature of the cis ligand is *less* than that for the trans ligand. An equation of this general form can be shown to hold exactly if the barrier height is approximated to Δ. In this case at temperature T for eq 31

$$k/n = A(\alpha)^m(\beta)^p \quad (31)$$

we simply derive

$$\log A = \log (\text{constant}) - \frac{[{}^1/_2(H_2O)_\sigma - (Cl)_\sigma]}{RT} \quad (32)$$

$$\log \alpha = \frac{(Cl)_\sigma - (NH_3)_\sigma}{RT} \qquad \log \beta = \frac{{}^1/_2(NH_3)_\sigma - {}^1/_2(Cl_3)_\sigma}{RT} \quad (33)$$

where $(H_2O)_\sigma$, $(Cl)_\sigma$, and $(NH_3)_\sigma$ are the $\beta_\sigma S_\sigma^2$ values for the relevant ligands. On this model α, β should be less than and greater than unity respectively and the cis effects should in general be less important than the trans effect. This is generally true from a selection of data in Table VII. We may fit our calculated barrier heights (sum of entering and leaving barriers) to an equation of the form

$$H = x + my + pz \quad (34)$$

with an rms deviation of 0.2 which is approximately the size of the scatter of points in Figure 8. $y = -0.084 \pm 0.01$ μm^{-1} and $z = 0.168 \pm 1.7$ μm^{-1} which are exactly in the ratio of −1:2. (1.0 μm^{-1} = 10 kK.)

Finally this set of examples is one where although the trans-labilizing effect of Cl^- is greater than that of NH_3 (rate *trans*-$Pt(NH_3)_2Cl_2$ > *cis*-$Pt(NH_3)_2Cl_2$ and the rate cis labilization of $PtNH_3Cl_3^-$ > trans labilization) it is the Cl^- ligand that is lost and not the NH_3. Note in this context that whereas from Table I $\beta_\sigma S_\sigma^2(NH_3) > \beta_\sigma S_\sigma^2(Cl^-)$ the $n_{Pt}{}^0$ values (Table IV) are almost identical ($3.07(NH_3) > 3.04(Cl^-)$). There are obviously subtle features of these substitution processes which lie beyond the explanation of the present work. The inquisitive reader will find more.

Hydrolysis and Anation of $Pt(DMSO)(H_2O)_xCl_{3-x}$

Elding has recently studied[76] the substitution reactions of $Pt(DMSO)(H_2O)_xCl_{3-x}$ systems with both Cl^- and H_2O as entering ligands. The relative ordering of the rate constants for this sequence of reactions turns out to be quite different from that for the analogous $Pt(NH_3)(H_2O)_xCl_{3-x}$ series we analyzed above. This is ascribed to the greater trans effects of the DMSO (S bonded) ligand compared to NH_3 or Cl^-. We have no $\beta_\sigma S_\sigma^2$ value for this ligand however but suspect that it will be a poor σ donor and similar to I^-. However, using eq 12 and leaving out values for Y_π and Y_s (which are unavailable to us), Elding's data are well fitted with a value of $\beta_\sigma S_\sigma^2 = 0.223$ μm^{-1} (Figure 11a) for the hydrolysis reactions. Transferring this value to the series of anation reactions also gives a good fit (Figure 11b) although two pairs of rate constants k_{-3}, k_{-4} and k_{-6}, k_{-7} are reversed. This value of $\beta_\sigma S_\sigma^2$, smaller than any in Table I, indeed fits in with ideas that DMSO (S bonded) is a better trans-effect ligand than Cl^-, H_2O, or NH_3. The agreement indicated by Figure 11 is as good as that found for the other systems we have looked at above and suggests that any π effects of DMSO as a ligand do not figure prominently in the reaction rates. Recall that our model suggests that the σ effects only of the ligands coordinated in the square-planar substrate are important.

The Success of the Model

In general the good correlation between calculated barrier heights and log (k/n) strongly supports the form of the d-orbital part of eq 11 in terms of ligand σ strengths. Previous molecular orbital ideas on the nature of the trans effect therefore need to be considerably updated to be able to rationalize a lot of the features of these replacement reactions. The new approach is quite successful in its global view of these processes. We see a larger change in rate constant between k_{2c} and k_{3c} than between k_1 and k_{2c} of Figure 7, indicating a larger susceptibility to ligand changes at the X or T positions than at the cis position. In addition, the effect of replacing Cl by H_2O is in the opposite direction in the cis position than in the X or T position. What is also shown very clearly from our plots of Figures 7–11 is that the rate decreases with increasing σ strength of the X or T positions but increases with increasing σ strength at the C_1 and C_2 positions. In conclusion it is useful to summarize our results as follows.

If the incoming barrier is rate determining as seems to be the case with most examples, then the following hold. (a) The barrier height decreases and thus rate of reaction increases with (i) increasing σ strength of the entering ligand, (ii) π-acceptor orbitals on the entering ligand, (iii) good interaction with $(n+1)$s,p orbitals on metal by the entering ligand, (iv) entering ligand "softness", (v) decreasing σ strength of the trans ligand (trans labilizing influence), (vi) decreasing σ strength of the leaving ligand, and (vii) increasing σ strength of cis ligands (cis effect). (b) The relative leaving barrier heights determine which ligand is lost from the tbp inter-

Table VII. Susceptibility of Rate Constant to Cis and Trans Ligands[a]

Metal	Entering ligand	Ligands X, T	α^b	β^b
Pt	H_2O	Cl, Cl	3×10^{-3}	3
Pt	H_2O	Br, Br	3×10^{-4}	6
Pt	H_2O	Cl, NH_3	0.5	2.4
Pd	NH_3	Cl, NH_3	0.1	10

[a] Data from ref 9. [b] From the relationship $\log k/n = A(\alpha)^m(\beta)^p$.

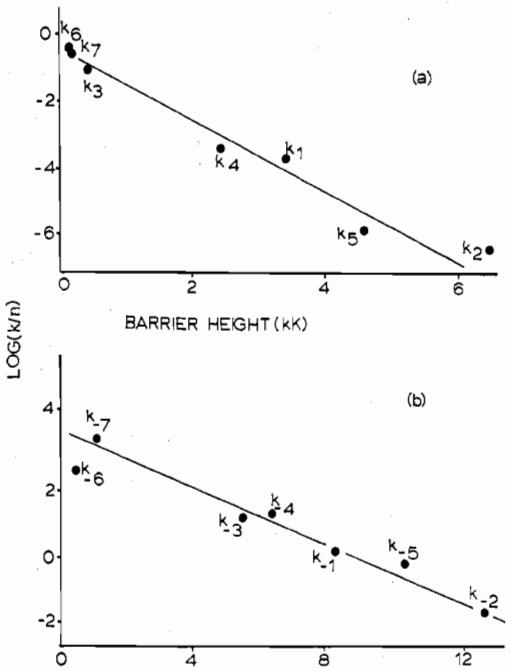

Figure 11. Calculated barrier height vs. observed log (statistical rate constant) for (a) hydrolysis and (b) anation of $Pt(DMSO)(H_2O)_xCl_{3-x}$ species, using a value of 0.223 μm^{-1} for $\beta_\sigma S_\sigma^2$ for the DMSO ligand.

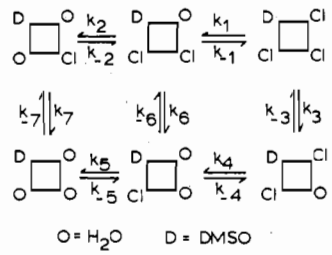

Figure 12. Reaction scheme for hydrolysis and anation of $Pt(DMSO)_x(H_2O)_xCl_{4-x-y}$ species.

mediate. Barrier height increases (and therefore trans-directing influence increases) with (i) decreasing σ-donor strength of the trans ligand, (ii) π-acceptor strength of the trans ligand, (iii) good interaction of the trans ligand with (n + 1)s,p orbitals on the metal, and (iv) "softness" of the trans ligand.

Some Comments on the Model

Our theory presented here is a very simple one. We have neglected effects which are of known importance in selected systems—solvation and steric effects for example.

One molecular orbital approximation we have used concerns the validity of ligand additivity, i.e., whether eq 5 is a good representation of the interaction energy in low-symmetry situations. As we have seen, good results were obtained for the log rate vs. barrier height plots for reaction of $Pt(H_2O)_xCl_{4-x}$ complexes where the σ strength of H_2O is 50% higher than that of Cl^-. Also the results with the DMSO-containing systems could be understood even though the σ strength of H_2O was calculated to be $\sim$3.5 times that of DMSO. This means that the assumption of ligand additivity makes little qualitative difference to the model at its present level of sophistication.

On the simple model presented here, the stabilization afforded by interaction of a coordinated ligand with metal (n + 1)s,p orbitals remains invariant in four- and five-coordinate structures. Changes in this sort of interaction have figured largely in previous semiquantitative molecular orbital approaches. They turn up in higher order approximations to our theoretical model. How important they are is a very difficult question to answer and again is related to whether the ligand additivity assumptions of our scheme are valid. It is also related to the whole problem of unravelling the role of higher energy orbitals in general (d orbitals in main-group and s,p orbitals in transition-metal chemistry). However, the changes in (n + 1)s,p interaction on going from substrates to tbp intermediate calculated for a limited number of systems[16] follow the trans-effect order, and so inclusion of this effect tends to reinforce the conclusions we have come to above.

In many ways therefore our molecular-orbital scheme is somewhat gross and it is perhaps surprising that we have been able to rationalize such a large amount of the available kinetic material on such a simple approach.

Acknowledgment. I would like to thank Professor M. L. Tobe and Dr. J. C. Lockhart for enlightening discussions and Dr. L. I. Elding for kindly allowing me to use his DMSO results prior to publication.

Registry No. $PtCl_4^{2-}$, 13965-91-8; $Pt(NH_3)Cl_3^-$, 17632-41-6; *cis*-$Pt(NH_3)_2Cl_2$, 15663-27-1; *trans*-$Pt(NH_3)_2Cl_2$, 14913-33-8; $Pt(NH_3)_3Cl^+$, 23678-44-6; $Pt(DMSO)Cl_3^-$, 31203-96-0; Cl^-, 16887-00-6; py, 110-86-1; NO_2^-, 14522-82-8; Br^-, 24959-67-9; I^-, 20461-54-5; SCN^-, 302-04-5; Ph_3Sb, 603-36-1; CN^-, 57-12-5; Ph_3P, 603-35-0.

References and Notes

(1) F. Basolo and R. G. Pearson, "Mechanism of Inorganic Reactions", Wiley, New York, N.Y., 1967.
(2) C. H. Langford and H. B. Gray, "Ligand Substitution Processes", W. A. Benjamin, New York, N.Y., 1965.
(3) F. Basolo, *Adv. Chem. Ser.*, **No. 49**, 81 (1965).
(4) J. O. Edwards, "Inorganic Reaction Mechanisms", W. A. Benjamin, New York, N.Y., 1964.
(5) L. Cattalini, *Prog. Inorg. Chem.*, **13**, 263 (1970).
(6) L. Cattalini, *MTP Int. Rev. Sci.: Inorg. Chem., Ser. One* (1972).
(7) J. S. Coe, *MTP Int. Rev. Sci.: Inorg. Chem., Ser. Two* (1974).
(8) M. L. Tobe, "Inorganic Reaction Mechanisms", Nelson, London, 1972.
(9) F. R. Hartley, *Chem. Soc. Rev.*, **2**, 163 (1973).
(10) F. Basolo and R. G. Pearson, *Prog. Inorg. Chem.*, **4**, 381 (1962).
(11) D. S. Martin, *Inorg. Chim. Acta, Rev.*, **1**, 87 (1967).
(12) A. Pidcock, R. E. Richards, and L. M. Venanzi, *J. Chem. Soc.* A, 1707 (1966).
(13) U. Belluco, M. Graziani, and P. Rigo, *Inorg. Chem.*, **5**, 1123 (1966).
(14) This is of course similar to the profile associated with the tbp transition state involved in nucleophilic substitution processes at tetrahedral carbon.
(15) R. McWeeny, R. Mason, and A. D. C. Towel, *Discuss Faraday Soc.*, **47**, 20 (1969).
(16) S. S. Zumdahl and R. S. Drago, *J. Am. Chem. Soc.*, **90**, 6669 (1968).
(17) D. R. Armstrong, R. Fortune, and P. G. Perkins, *Inorg. Chim. Acta*, **9**, 9 (1974).
(18) L. E. Orgel, *J. Inorg. Nucl. Chem.*, **2**, 137 (1956).
(19) J. Chatt, L. A. Duncanson, and L. M. Venanzi, *J. Chem. Soc.*, 4456 (1955).
(20) L. G. Vanquickenborne, J. Vrankx, and C. Göller-Walrand, *J. Am. Chem. Soc.*, **96**, 4121 (1974).
(21) J. Vrankx and L. G. Vanquickenborne, *Inorg. Chim. Acta*, **11**, 159 (1974).
(22) C. E. Schaffer and C. K. Jørgensen, *Mol. Phys.*, **9**, 401 (1965).
(23) C. E. Schaffer, *Struct. Bonding (Berlin)*, **14**, 69 (1973).
(24) S. F. A. Kettle, *J. Chem. Soc. A*, 420 (1966).
(25) J. K. Burdett, *Inorg. Chem.*, **14**, 375 (1975).
(26) We assume in fact that the ligand field is additive in low-symmetry situations where the ligands are different. See ref 21, 28, and 29a for a more general discussion of the problem.
(27) W. Smith and D. W. Clack, *Rev. Roum. Chim.*, **20**, 1243 (1975).
(28) M. Gerloch and R. C. Slade, "Ligand Field Parameters" Cambridge University Press, New York, N.Y., 1973.
(29) (a) J. Glerup, O. Mønsted, and C. E. Schäffer, *Inorg. Chem.* **15**, 1399 (1976). (b) A rival σ bonding order is given in J. R. Perumareddi, *Coord. Chem. Rev.*, **4**, 73 (1969). (c) In referring to σ strengths of ligands in this paper we shall follow the order of Table I. We point out here that this may not be the same as the qualitative σ-donor strength order reached by other routes.
(30) J. K. Burdett, *Inorg. Chem.*, **15**, 212 (1976).
(31) J. K. Burdett, *J. Chem. Soc., Dalton Trans.*, 1725 (1976).
(32) Reference 2, p 25.
(33) E.g., C. S. G. Philips and R. J. P. Williams, "Inorganic Chemistry", Oxford University Press, London, 1966.
(34) One possible reason for using the LFAC rather than the molecular-orbital approach (but one we do not advocate) is that with the former, the tbp always lies to higher energy than the planar substrate. Use of the barycentered orbital set gave negative activation energies however when applied to the octahedral substitution problem (see ref 31).
(35) C. D. Falk and J. Halpern, *J. Am. Chem. Soc.*, **87**, 3003 (1965).
(36) J. K. Burdett, *Inorg. Chem.*, **14**, 931 (1975).
(37) See, for example, S. Glasstone, K. J. Laidler, and H. Eyring, "Theory of Rate Processes", McGraw-Hill, New York, N.Y., 1941.
(38) L. Cattalini, G. Marangoni, S. Degetto, and M. Brunelli, *Inorg. Chem.*, **10**, 1545 (1971).
(39) A. A. Grinberg and L. E. Nikolskoya, *Zh. Prikl. Khim. (Leningrad)*, **22**, 542 (1949); **24**, 893 (1951).
(40) L. Cattalini, A. Orio, and A. Doni, *Inorg. Chem.*, **5**, 1517 (1966).
(41) L. Cattalini, G. Marangoni, and M. Martelli, *Inorg. Chem.*, **7**, 1495 (1968).
(42) R. Romeo and M. L. Tobe, *Inorg. Chem.*, **13**, 1991 (1974).
(43) P. D. Braddock, R. Romeo, and M. L. Tobe, *Inorg. Chem.*, **13**, 1170 (1974).
(44) M. L. Tobe, unpublished data.
(45) K. N. Raymond, P. W. R. Corfield, J. A. Ibers, *Inorg. Chem.* **7**, 842 (1968).
(46) J. O. Edwards and R. G. Pearson, *J. Am. Chem. Soc.*, **84**, 16 (1962).
(47) D. M. P. Mingos, *Nature (London), Phys. Sci.*, **229**, 193 (1971).
(48) L. Cattalini, M. Martelli, and P. Rigo, *Inorg. Chim. Acta*, **1**, 149 (1967).
(49) U. Belluco, E. Ettore, F. Basolo, R. G. Pearson, and A. Turco, *Inorg. Chem.*, **5**, 591 (1966).
(50) L. Cattalini and M. Martelli, *Gazz. Chim. Ital.*, **97**, 488 (1967).
(51) U. Belluco, M. Graziani, M. Nicolini, and P. Rigo, *Inorg. Chem.*, **6**, 721 (1967).
(52) See, for example, ref 5.
(53) E. L. Muetterties, Ed., "Transition Metal Hydrides", Marcel Dekker, New York, N.Y., 1971.
(54) More detailed molecular orbital arguments (ref 55) show that for this d^8 system the best σ donors will occupy axial sites in the trigonal bipyramid. Also π acceptors prefer equatorial and π donors axial positions in the tbp.
(55) A. R. Rossi and R. Hoffmann, *Inorg. Chem.*, **14**, 365 (1975).
(56) A. W. Adamson, *J. Phys. Chem.*, **71**, 798 (1967).
(57) M. Martelli and A. Orio, *Ric. Sci.*, **35**, 1089 (1962).
(58) Although from the more complete molecular orbital considerations of ref 55 the phosphine would prefer an equatorial site in the trigonal bipyramid.
(59) U. Belluco, L. Cattalini, F. Basolo, R. G. Pearson, and A. Turco, *J. Am. Chem. Soc.*, **87**, 241 (1965).
(60) L. I. Elding, *Acta Chem. Scand.*, **24**, 1331 (1970).
(61) L. I. Elding, *Acta Chem. Scand.*, **24**, 1341 (1970).
(62) L. I. Elding, *Acta Chem. Scand.*, **24**, 1527 (1970).
(63) L. I. Elding, *Acta Chem. Scand.*, **24**, 2546 (1970).
(64) L. I. Elding, *Acta Chem. Scand.*, **24**, 2557 (1970).
(65) L. I. Elding, *Inorg. Chim. Acta*, **6**, 683 (1972).
(66) C. B. Colvin, R. G. Gunther, L. D. Hunter, J. A. McLean, M. A. Tucker, and D. S. Martin, *Inorg. Chim. Acta*, **2**, 487 (1968).
(67) R. A. Rheinhardt and W. W. Monk, *Inorg. Chem.*, **9**, 2026 (1970).
(68) R. A. Rheinhardt and R. K. Sparkes, *Inorg. Chem.*, **6**, 2190 (1967).
(69) J. W. Reishus and D. S. Martin, *J. Am. Chem. Soc.*, **83**, 2457 (1961).

(70) T. S. Ellerman, J. W. Reishus, and D. S. Martin, *J. Am. Chem. Soc.*, **80**, 536 (1958).
(71) T. S. Elleman, J. W. Reishus, and D. S. Martin, *J. Am. Chem. Soc.*, **81**, 10 (1959).
(72) L. F. Grantham, T. S. Elleman, and D. S. Martin, *J. Am. Chem. Soc.*, **77**, 2965 (1955).
(73) F. Aprile and D. S. Martin, *Inorg. Chem.*, **1**, 551 (1962).
(74) M. A. Tucker, C. B. Colvin, and D. S. Martin, *Inorg. Chem.*, **3**, 1373 (1964).
(75) D. Bannerjea, F. Basolo, and R. G. Pearson, *J. Am. Chem. Soc.*, **79**, 4055 (1957).
(76) L. I. Elding, unpublished results.

Contribution from the Chemistry Division,
Naval Research Laboratory, Washington, D.C. 20375

Determination of the Vapor Pressure and Vaporization Coefficient of Polymeric Sulfur Nitride, $(SN)_x$

DAVID C. WEBER*[1] and CURTIS T. EWING

Received April 7, 1977 AIC70254I

The vapor pressure and vaporization coefficient of $(SN)_x$ were determined in the range 100–150 °C by a modification of the direct Knudsen method. Saturation pressures were derived from undersaturation information by a correlation and extrapolation of flux results from a single Knudsen cell with different orifice sizes. The vapor pressure of $(SN)_x$ is represented by $\ln P = 37.64 - 16351/T$. Enthalpy of vaporization is 32.49 ± 0.99 kcal/(mol K) and the vaporization coefficient 0.0035 ± 0.0004.

Introduction

Recent investigations[2,3] of the "nonmetallic" metal $(SN)_x$ have created considerable interest in the scientific community. The main emphasis has been on the conducting properties of the material and on the mechanism of conduction, but many physical and chemical studies have also been made. Smith et al.[4] have recently shown with mass spectrometric techniques that the vapor formed in the sublimation process is composed almost entirely of one species corresponding stoichiometrically to $(SN)_4$ but differing structurally from the "cradlelike" S_4N_4. Bright et al.[3,5] had shown that the polymeric $(SN)_x$ could be sublimed and recondensed to yield films of $(SN)_x$ similar in properties and appearance to the original bulk material. This phenomenon is of considerable interest since polymers generally do not behave in this manner.

The determination of the vapor pressure and the vaporization coefficient of $(SN)_x$ is a logical extension of these prior studies and sheds some light on the processes involved in vaporization. The vaporization coefficient is generally very small for materials when the molecular structure of the vapor species is substantially different from that of the bulk phase. This situation was found to be true for $(SN)_x$ and the unusually low vaporization coefficient generated some interesting but unique problems in the determination of saturation pressure.

Theory

The determination of vapor pressure by the Knudsen method is well-known for systems in which the pressure in the cell has reached saturation. Where this is not the case, saturation pressure (P_e) is related to the observed pressure (P_o) at varying degrees of undersaturation by the classical equation

$$P_e = P_o[1 + A_o/\alpha A_1] \quad (1)$$

where A_o is orifice area, A_1 is evaporating area, and α is vaporization coefficient. This equation was derived for a cylindrical cell with the sample located at the base and an orifice located coaxially at the top of the cell. It was assumed in the derivation that the pressure is constant throughout the cell.

A generally more acceptable form is that derived by Motzfeldt[6]

$$P_o = P_e/\left[1 + \frac{A_o}{A_1}\left(\frac{1}{\alpha} + \frac{1}{K} - 2\right)\right] \quad (2)$$

where K is the Clausing factor[7] of the cell. This Clausing factor is related to the theoretical value (K_T) by[8]

$$K = K_T \sum_{n=0}^{\infty} [(1 - K_T)(1 - \alpha)]^n \quad (3)$$

It can be readily shown that when α is very small, the effective Clausing factor, K, will be ~1 and eq 2 approaches the form of eq 1. This then permits the application of the classical form of the equation when determining P_e for materials with low vaporization coefficients.

For many materials α is near unity and saturation can be achieved by the appropriate selection of cell and orifice sizes so that as the ratio $A_o/\alpha A_1$ approaches zero, P_o approaches P_e. If, however, the vaporization coefficient is very small, it becomes impractical to construct a cell which allows one to reach saturation within the cell. For this case, it is feasible at a particular temperature to obtain P_e indirectly[9] by determining values of P_o for differing degrees of undersaturation (different orifice sizes) and extrapolating these values with eq 1 to the saturation condition.

Experimental Section

Vaporization rates for $(SN)_x$ were obtained isothermally with small Knudsen cells by measuring weight loss against time with a recording Mettler thermoanalyzer[10] (Table I). All runs were carried out under apparent vacuums of 10^{-5} Torr or better.

Within the Mettler system, the Knudsen cell was positioned on top of a two-hole ceramic tube containing the thermocouple in such a way that the base of the cell was in direct contact with the hot junction of the thermocouple. Equilibrium temperature readings from this couple were observed with a precision potentiometer independently of the Mettler system. The calibration of the platinum—platinum–10% rhodium thermocouples was taken to be the same as that obtained by direct calibration at NBS for couples from the same rolls of wire. The isothermality of the furnace area was ensured by extensive testing in previous work with the thermoanalyzer.[11] The balance was frequently calibrated with standard weights and the chart speed was periodically checked; no calibration or adjustment of either was necessary.

The material used for this study was prepared at NRL using the method described by Mikulski et al.[12] A mass spectral analysis of the $(SN)_x$ used in this study was found to be the same as that for University of Pennsylvania material which was prepared by the same method and shown by commercial analysis[12] to be analytically pure. The material from the two sources is believed to be identical.

The $(SN)_x$ was loaded into the Knudsen cell under an inert atmosphere. The cell was generally filled to within $^1/_{16}$ in. of the top